

Chiral Effects and Cosmic Magnetic Fields

Hiroyuki Tashiro, Tanmay Vachaspati
Physics Department, Arizona State University, Tempe, AZ 85287, USA.

Alexander Vilenkin
*Institute of Cosmology, Department of Physics & Astronomy,
212 College Avenue, Tufts University, Medford, MA 02155, USA.*

(Dated: February 20, 2022)

In the presence of cosmic chiral asymmetry, chiral-vorticity and chiral-magnetic effects can play an important role in the generation and evolution of magnetic fields in the early universe. We include these chiral effects in the magnetic field equations and find solutions under simplifying assumptions. Our numerical and analytical results show the presence of an attractor solution in which chiral effects produce a strong, narrow, Gaussian peak in the magnetic spectrum and the magnetic field becomes maximally helical. The peak in the spectrum shifts to longer length scales and becomes sharper with evolution. We also find that the dynamics may become non-linear for certain parameters, pointing to the necessity of a more complete analysis.

I. INTRODUCTION

Cosmic relics, such as topological defects and magnetic fields, can be used as probes of the very early universe and extremely high energy particle physics. The formation, evolution, and observational signatures of topological defects have been studied for over three decades, and constraints have been obtained that have guided particle physics model building. The formation of magnetic fields during cosmological phase transitions has also been investigated [1–3]. Current observational constraints are relatively weak, allowing for intergalactic magnetic field strengths at the nano Gauss level (see for example, [4–8]).

An attractive scenario links the generation of magnetic fields to the generation of the observed matter-antimatter asymmetry [9–12]. The produced magnetic field carries magnetic helicity that is directly proportional to the baryon number density [9, 10]

$$h = -\kappa \frac{n_b}{\alpha}, \quad (1)$$

where α is the fine structure constant, $\kappa \approx 0.01$ [11, 12], and

$$h = \frac{1}{V} \int_V d^3x \mathbf{A} \cdot \mathbf{B}, \quad (2)$$

is the magnetic helicity density and n_b is the baryon number density. The minus sign in the relation (1) is a direct cosmological manifestation of CP violation in particle physics that also gives preference to matter over antimatter in the universe. The injection of helical magnetic fields into the plasma can transfer magnetic field power to larger length scales by the “inverse cascade”, providing hope that even small scale magnetic fields from phase transitions can grow to astrophysically relevant scales at more recent epochs. *Helical* magnetic fields can possibly be detected through various cosmological observations [13–15].

Two important chiral effects, called the chiral-vorticity ($\chi\omega$) [16] and chiral-magnetic (χB) [17] effects, can also play a role in the early universe [18] and in QCD [19, 20]. To understand these effects, consider Fig. 1 where we show the effect of a magnetic field on, for example, electrons. The magnetic field couples to the magnetic moments and tends to align them. Depending on the electric charge of the carrier, the spins are either aligned or anti-aligned with the magnetic moment. The helicity eigenstates of the fermions then determine the direction of the momentum of the particles, which in turn gives the direction of the electric current due to each species. Taking the left- and right-handed electrons and positrons as the four fermion states, which we assume to be massless, we see that the net electric current is

$$J_{\chi B} \propto [n(e_L^-) - n(e_R^+)] - [n(e_R^-) - n(e_L^+)], \quad (3)$$

where $n(e_L^-)$ denotes the number density of e_L^- and similarly for the other particle species. In terms of the chemical potentials for left- and right-handed electrons, the differences within the square brackets are given by μ_L and μ_R respectively. So $J_{\chi\omega} \propto \Delta\mu \equiv \mu_L - \mu_R$. The calculation in Ref. [17] gives

$$\mathbf{J}_{\chi B} = \frac{e^2}{2\pi^2} \Delta\mu \mathbf{B}. \quad (4)$$

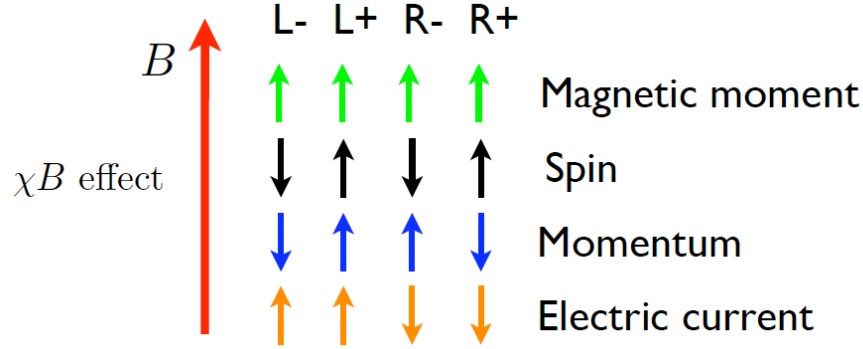


FIG. 1: Understanding the χB effect. An external magnetic field tends to align the magnetic moments of the four electron states – left-right handedness for electron and positron, denoted in the figure as $L+$, $L-$, $R+$, $R-$ – which implies the shown directionalities of the spin, momenta, and electric current due to each state. If the four states are present in unequal numbers, net electric current may be induced.

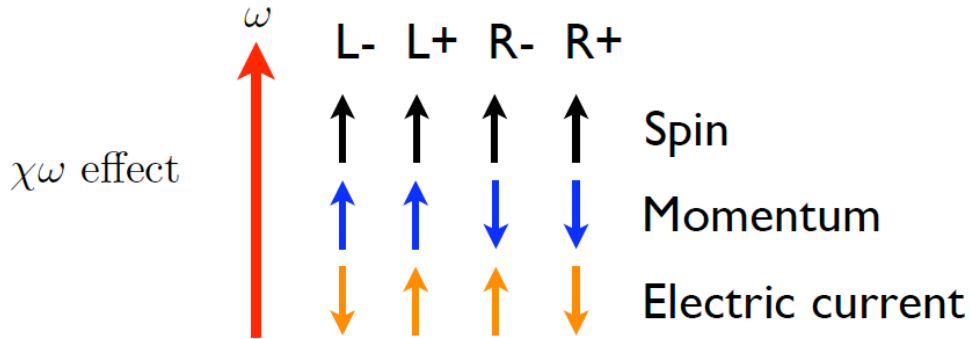


FIG. 2: Understanding the $\chi\omega$ effect. Vortical fluid flow tends to align the spins of the four electron states which implies the shown directionalities of the momenta and electric current due to each state. If the four states are present in unequal numbers, net electric current may be induced.

Similarly, in Fig. 2, we explain the $\chi\omega$ effect, which occurs if the ambient fluid flow has vorticity (ω). Spin-orbit coupling tends to align the spins of the fermions; particle helicity then aligns the left-handed states but anti-aligns the right-handed states, which leads to the electric currents as shown. Thus, in equilibrium,

$$J_{\chi\omega} \propto [n(e_L^-) + n(e_R^+)] - [n(e_R^-) + n(e_L^+)]. \quad (5)$$

The presence of non-zero μ_L means that $n(e_L^-) \neq n(e_R^+)$ and of μ_R that $n(e_R^-) \neq n(e_L^+)$. However, if $\mu_L = \mu_R$ then $n(e_L^-) = n(e_R^-)$ and $n(e_R^+) = n(e_L^+)$, and $J_{\chi\omega}$ vanishes. Also if $\mu_L = -\mu_R$ then $n(e_L^-) = n(e_L^+)$ and $n(e_R^+) = n(e_R^-)$, and again $J_{\chi\omega} = 0$. So for $J_{\chi\omega}$ to be non-vanishing, we need $\Delta\mu^2 \equiv \mu_L^2 - \mu_R^2 \neq 0$. The exact calculation in Ref. [16] gives

$$\mathbf{J}_{\chi\omega} = \frac{e}{4\pi^2} \Delta\mu^2 \boldsymbol{\omega}, \quad (6)$$

where $\boldsymbol{\omega} = \nabla \times \mathbf{v}$ is the fluid vorticity.

The above expression for $\mathbf{J}_{\chi\omega}$ holds when the left- and right-handed particles and antiparticles are in thermal equilibrium at the same temperature. If some of the species are at different temperatures there is an additional contribution per species to $\mathbf{J}_{\chi\omega}$ proportional to $eT^2\boldsymbol{\omega}$ where T is the temperature of the particular species [16]. We will not consider this situation in the present paper, though it may be important for the contribution of left- and right-handed particles, especially neutrinos, to the hypercharge current in the epoch before electroweak symmetry breaking.

The χB and $\chi\omega$ effects can only lead to a non-zero electric current if there is a disbalance between left- and right-handed particles, that is, $\Delta\mu \neq 0$. Such a disbalance can arise in the early universe from out-of-equilibrium P -violating

decays of massive particles. For example, it could arise due to inflaton decay at the end of inflation. The resulting values of $\Delta\mu$ are not generally suppressed by any small couplings, so large values like $\Delta\mu/T \sim 0.1 - 1$ can easily be achieved [21, 22]. A right-left asymmetry is also likely to be created during leptogenesis, if it occurs at some energy scale much higher than the electroweak scale. In particular, an asymmetry between left- and right-handed electrons will be created because they carry different charges under the electroweak symmetry group $SU(2)_L \times U(1)_Y$. The chirality-flipping processes due to nonzero electron mass are suppressed at high temperatures, and this asymmetry is preserved until the temperature drops below $T_f \sim 80$ TeV [23]. If vorticity develops at any temperature higher than T_f , the $\chi\omega$ effect will operate and create a magnetic field. Since the electroweak symmetry is unbroken, this magnetic field will be the $U(1)$ hypercharge magnetic field, and will get converted to electromagnetic magnetic field after the electroweak phase transition.

It is worth noting that chiral effects induce kinetic and magnetic helicities even if these are not present initially. For the $\chi\omega$ effect, Fig. 2 shows that momenta tend to be aligned along ω , which means that $\mathbf{v} \cdot \omega \neq 0$ and so kinetic helicity is induced. In the case of the χB effect, if the magnetic field is helical, then the induced current, hence velocity, is along the magnetic field and the fluid flow carries kinetic helicity. This fact may be of interest if the kinetic helicity survives until recombination because then it can produce parity odd temperature-polarization correlations [24].

Once a magnetic field is generated, its subsequent evolution may also be influenced by chiral effects. In particular, Joyce and Shaposhnikov [22] have shown that χB currents can induce an exponential growth of the magnetic field on sufficiently large length scales. A helical magnetic field, in turn, back-reacts on the evolution of the left-right disbalance $\Delta\mu$. This is described by the chiral anomaly equation, which relates changes in $\Delta\mu$ to changes in magnetic helicity [22],

$$\frac{d(\Delta\mu)}{dt} = -\frac{c_\Delta \alpha}{T^2} \frac{dh}{dt} - \Gamma_F \Delta\mu. \quad (7)$$

Here, Γ_F is the chirality-flipping rate and $c_\Delta \sim 1$, α is the fine structure constant, and T is the temperature at time t . Boyarsky et al [25] have shown that as a result the left-right disbalance can survive down to $T \sim 10$ MeV if helical magnetic fields are present, for example due to baryogenesis.

The plasma equations in the radiation-baryon single fluid approximation are

$$\partial_t \rho + \frac{4}{3} \nabla \cdot (\rho \mathbf{v}) = 0, \quad (8)$$

$$\frac{4}{3} \partial_t (\rho \mathbf{v}) - \frac{4}{3} \rho \mathbf{v} \times (\nabla \times \mathbf{v}) = \mathbf{J} \times \mathbf{B} - \nabla p, \quad (9)$$

$$\nabla \times \mathbf{B} = \mathbf{J}, \quad (10)$$

$$\nabla \times \mathbf{E} = -\partial_t \mathbf{B}, \quad (11)$$

where we have used natural units, $\hbar = 1 = c$. The fluid density is ρ , the pressure is p . The displacement current has been ignored, as is done in magnetohydrodynamics (MHD) when the flow velocities are small compared to the speed of light. Since we are mainly focusing on chiral effects, we have simplified the equations by ignoring the injection of magnetic fields by external sources such as sphalerons [10], and the dissipative effects of viscosity. Cosmological expansion can be included in the Maxwell equations by going to conformal coordinates, as we will do in Sec. II.

The electric current is given by the sum of the Ohmic and chiral components

$$\mathbf{J} = \mathbf{J}_{\text{Ohm}} + \mathbf{J}_{\chi\omega} + \mathbf{J}_{\chi B}. \quad (12)$$

The Ohmic component is given by

$$\mathbf{J}_{\text{Ohm}} = \sigma(\mathbf{E} + \mathbf{v} \times \mathbf{B}). \quad (13)$$

where σ is the electrical conductivity of the plasma. The chiral components, $\mathbf{J}_{\chi B}$ and $\mathbf{J}_{\chi\omega}$, are given in Eqs. (4) and (6), together with the chiral anomaly equation in the form of Eq. (7).

In Eq. (11) we can replace \mathbf{E} by the currents and with a little algebra we find

$$\partial_t \mathbf{B} = \nabla \times (\mathbf{v} \times \mathbf{B}) + \gamma_D \nabla^2 \mathbf{B} + \gamma_\omega \nabla \times \omega + \gamma_B \nabla \times \mathbf{B}, \quad (14)$$

where

$$\gamma_D = \frac{1}{\sigma}, \quad \gamma_\omega = \frac{e\Delta\mu^2}{4\pi^2\sigma}, \quad \gamma_B = \frac{e^2\Delta\mu}{2\pi^2\sigma} \quad (15)$$

The terms on the right-hand side of (14) will be referred to as the advection, diffusion, $\chi\omega$, and χB terms respectively. The above set of equations exhibits all the complexities of MHD plus those arising from the chiral anomaly.

It is helpful to compare order of magnitudes of the various terms on the right-hand side of Eq. (14). If L denotes a length scale of interest, the advection, diffusion, $\chi\omega$ and χB terms are estimated as

$$\nabla \times (\mathbf{v} \times \mathbf{B}) \sim \frac{vB}{L}, \quad \gamma_D \nabla^2 \mathbf{B} \sim \frac{B}{\sigma L^2}, \quad \gamma_\omega \nabla \times \boldsymbol{\omega} \sim \frac{e\Delta\mu^2 v}{\sigma L^2}, \quad \gamma_B \nabla \times \mathbf{B} \sim \frac{e^2 \Delta\mu B}{\sigma L}. \quad (16)$$

Assuming that $\mu_L \sim \mu_R \sim T$ and using $\sigma \sim T/e^2$ [26, 27], the estimates for the four terms become vB/L , $e^2 B/(TL^2)$, $e^3 vT/L^2$, and $e^4 B/L$ respectively. Now for small flow velocities, $v \ll \max\{e^2/(TL), e^4\}$, or small magnetic fields, $B \ll e^3 T/L$, the advection term is subdominant and can be ignored. The second case we consider is when the length scale is large and the magnetic field is small: $L \gg \min\{e^2/(vT), 1/(e^2 T)\}$, $B \ll evT^2$. Then the diffusion term can be neglected.

We solve the evolution equations in an expanding spacetime, first numerically in Sec. IIC and then analytically in Sec. IID. Throughout this analysis we adopt some simplifications. First of all, we do not attempt to solve the fluid dynamics equations and represent the velocity field by a mode distribution with a Kolmogorov spectrum and fixed phases. (A more realistic representation of turbulent dynamics would include time variation of the phases.) We also assume negligible advection; the consistency of the latter assumption is discussed in Sec. IID. Our conclusions are summarized and discussed in Sec. III. In particular, we argue that under certain conditions the magnitude and the spectrum of the magnetic fields produced by our mechanism are not sensitive to the details of the turbulent velocity flow. Our estimates should then be valid, despite the oversimplified treatment of turbulent dynamics. In Appendix A we also consider steady-state solutions, *i.e.* with $\partial_t \mathbf{B} = 0$, in the regimes of negligible advection and of negligible diffusion in Minkowski spacetime.

II. MAGNETIC FIELD GENERATION AND EVOLUTION

As discussed at the end of Sec. I, there is a range of conditions within which the advection term may be dropped. Without the advection term, Eq. (14) is linear in \mathbf{v} and \mathbf{B} , and a mode expansion converts the equation into a set of ordinary differential equations. However, the dynamics is still highly non-trivial because of the mode coupling that arises due to the evolution of $\Delta\mu$, as the magnetic helicity on the right-hand side of Eq. (7) is an integral over all modes. Here we shall assume that advection is negligible. The validity of this assumption will be discussed at the end of Sec. IID.

A complete analysis, which is beyond the scope of the present paper, would need to include the evolution of the velocity field which is governed by the Navier-Stokes equation. Here we will consider the simpler case of incompressible, turbulent flows, with a specified distribution of velocities. These assumptions are valid when the magnetic field energy density is much smaller than the kinetic energy of the fluid and we can ignore the backreaction of the magnetic field on the fluid flow.

In a cosmological setting, we assume a flat Robertson-Walker metric

$$ds^2 = R^2(\eta)(-d\eta^2 + \delta_{ij} dx^i dx^j), \quad (17)$$

where $R(\eta)$ is the scale factor. It is convenient to choose $R(\eta)$ to have dimensions of length, and η , x^i to be dimensionless. The scale factor is related to cosmic temperature by $R = 1/T$. In the radiation dominated epoch, we also define the conformal time as $\eta = M_*/T$, where $M_* = \sqrt{90/8\pi^3} g_* M_{\text{P}}$ and $g_* \sim 100$ is the effective number of relativistic degrees of freedom. With this normalization, we find $\eta \sim 0.1$ when $T \sim M_{\text{P}}$ and, for example, $\eta \sim 10^{27}$ at matter-radiation equality when $T \sim 1$ eV. We also define comoving variables

$$B_c = R^2(\eta)B(\eta), \quad \Delta\mu_c = R(\eta)\Delta\mu, \quad (18)$$

and the comoving electrical conductivity is given by [27],

$$\sigma_c = R(\eta)\sigma = 70. \quad (19)$$

In these comoving variables, the magnetic field evolution Eq. (14) takes the form

$$\partial_\eta \mathbf{B}_c = \nabla_c \times (\mathbf{v}_c \times \mathbf{B}_c) + \gamma_{Dc} \nabla_c^2 \mathbf{B}_c + \gamma_{\omega c} \nabla_c \times (\nabla_c \times \mathbf{v}_c) + \gamma_{Bc} \nabla_c \times \mathbf{B}_c, \quad (20)$$

where $\gamma_{Dc} = 1/\sigma_c$, $\gamma_{\omega c} = e\Delta\mu_c^2/4\pi^2\sigma_c$, $\gamma_{Bc} = e^2\Delta\mu_c/2\pi^2\sigma_c$, ∇_c is differentiation with respect to the spatial metric δ_{ij} and \mathbf{v}_c is the comoving velocity. Note that $\mathbf{v}_c = \mathbf{v}$ by definition.

From Eq. (7), the evolution of the comoving chemical potential is given by

$$\frac{d\Delta\mu_c}{d\eta} = -c_\Delta \alpha \partial_\eta h_c - \Gamma_F \Delta\mu_c, \quad (21)$$

where h_c is $R^3 h$ and Γ_F is the chirality-flipping rate that we can ignore in the early universe $T > 80$ TeV [23]. In what follows we will always work with comoving quantities and will omit the subscript c for convenience.

A. Decomposition into modes

In order to solve for the evolution of the magnetic field with a chemical potential, we decompose the vector fields in the modes, \mathbf{Q}_i^\pm , which are divergence-free eigenfunctions of the Laplacian operator in comoving coordinates,

$$\mathbf{Q}^\pm(\mathbf{k}) = \frac{\mathbf{e}_1(\mathbf{k}) \pm i\mathbf{e}_2(\mathbf{k})}{\sqrt{2}} \exp(i\mathbf{k} \cdot \mathbf{x}), \quad (22)$$

where $\mathbf{e}_3 = \mathbf{k}/k$ and $(\mathbf{e}_1, \mathbf{e}_2, \mathbf{e}_3)$ form a right-handed, orthonormal triad of unit vectors. Then, $\nabla \cdot \mathbf{Q}^\pm = 0$ and $\nabla \times \mathbf{Q}^\pm = \pm k \mathbf{Q}^\pm$, and we also take $Q^{\pm*}(-\mathbf{k}) = Q^\pm(+\mathbf{k})$.

The velocity field of the incompressible ($\nabla \cdot \mathbf{v} = 0$) fluid is now decomposed in modes

$$\mathbf{v}(\eta, \mathbf{x}) = \int \frac{d^3k}{(2\pi)^3} [\tilde{v}^+(\eta, \mathbf{k}) \mathbf{Q}^+(\mathbf{k}) + \tilde{v}^-(\eta, \mathbf{k}) \mathbf{Q}^-(\mathbf{k})]. \quad (23)$$

The fluid kinetic energy density is given by

$$\frac{\rho_r}{2} \langle |\mathbf{v}(\eta, \mathbf{x})|^2 \rangle \equiv \frac{\rho_r}{2} \int d \log k E_V(\eta, k) = \rho_r \int \frac{k^2 dk}{(2\pi)^2} [|v^+(\eta, k)|^2 + |v^-(\eta, k)|^2], \quad (24)$$

where ρ_r is the radiation density, and we have taken statistically isotropic correlators,

$$\langle \tilde{v}^{\pm*}(\eta, \mathbf{k}) \tilde{v}^\pm(\eta, \mathbf{p}) \rangle = |v^\pm(\eta, k)|^2 (2\pi)^3 \delta^{(3)}(\mathbf{k} - \mathbf{p}) \quad (25)$$

$$\langle \tilde{v}^{+*}(\eta, \mathbf{k}) \tilde{v}^-(\eta, \mathbf{p}) \rangle = \langle \tilde{v}^{-*}(\eta, \mathbf{k}) \tilde{v}^+(\eta, \mathbf{p}) \rangle = 0. \quad (26)$$

Proceeding in the same way, the fluid helicity is

$$\langle \mathbf{v} \cdot \boldsymbol{\omega} \rangle \equiv \int d \log k H_V(\eta, k) = \int \frac{k^3 dk}{2\pi^2} [|v^+(\eta, k)|^2 - |v^-(\eta, k)|^2]. \quad (27)$$

The magnetic field is similarly decomposed

$$\mathbf{B}(\eta, \mathbf{x}) = \int \frac{d^3k}{(2\pi)^3} [\tilde{B}^+(\eta, \mathbf{k}) \mathbf{Q}^+(\mathbf{k}) + \tilde{B}^-(\eta, \mathbf{k}) \mathbf{Q}^-(\mathbf{k})]. \quad (28)$$

where the scalar mode is absent because $\nabla \cdot \mathbf{B} = 0$. The ensemble average of the magnetic field energy density is

$$\frac{1}{2} \langle |\mathbf{B}(\eta, \mathbf{x})|^2 \rangle \equiv \int d \log k E_B(\eta, k) = \int \frac{k^2 dk}{(2\pi)^2} [|B^+(\eta, k)|^2 + |B^-(\eta, k)|^2]. \quad (29)$$

where, just as for the velocity field,

$$\langle \tilde{B}^{\pm*}(\eta, \mathbf{k}) \tilde{B}^\pm(\eta, \mathbf{p}) \rangle = |B^\pm(\eta, k)|^2 (2\pi)^3 \delta^{(3)}(\mathbf{k} - \mathbf{p}) \quad (30)$$

$$\langle \tilde{B}^{+*}(\eta, \mathbf{k}) \tilde{B}^-(\eta, \mathbf{p}) \rangle = \langle \tilde{B}^{-*}(\eta, \mathbf{k}) \tilde{B}^+(\eta, \mathbf{p}) \rangle = 0. \quad (31)$$

The magnetic field helicity density is

$$\langle \mathbf{A} \cdot \mathbf{B} \rangle \equiv \int d \log k H_B(\eta, k) = \int \frac{k dk}{2\pi^2} [|B^+(\eta, k)|^2 - |B^-(\eta, k)|^2]. \quad (32)$$

and from Eq. (2) we have

$$\langle h \rangle = \langle \mathbf{A} \cdot \mathbf{B} \rangle. \quad (33)$$

The MHD equation, Eq. (20), without the advection term, can be decomposed into equations for the modes \tilde{B}^\pm

$$\partial_\eta \tilde{B}^+ = (-\gamma_D k^2 + \gamma_B k) \tilde{B}^+ + \gamma_\omega k^2 \tilde{v}^+, \quad (34)$$

$$\partial_\eta \tilde{B}^- = (-\gamma_D k^2 - \gamma_B k) \tilde{B}^- + \gamma_\omega k^2 \tilde{v}^-. \quad (35)$$

We multiply the first equation by \tilde{B}^{+*} and the second by \tilde{B}^{-*} and take ensemble averages to get

$$\partial_\eta |B^+|^2 = 2(-\gamma_D k^2 + \gamma_B k) |B^+|^2 + 2\gamma_\omega k^2 \langle \tilde{B}^{+*} \tilde{v}^+ \rangle, \quad (36)$$

$$\partial_\eta |B^-|^2 = 2(-\gamma_D k^2 - \gamma_B k) |B^-|^2 + 2\gamma_\omega k^2 \langle \tilde{B}^{-*} \tilde{v}^- \rangle. \quad (37)$$

The magnetic field is zero initially and only the $\chi\omega$ term is important on the right-hand side. Hence at early times, the solution to Eqs. (34) and (35) is

$$\tilde{B}^\pm(\eta, \mathbf{k}) = \gamma_\omega k^2 \int_{\eta_0}^{\eta} d\eta' \tilde{v}^\pm(\eta', \mathbf{k}) \quad (38)$$

Note that γ_ω is, in principle, a function of time since $\Delta\mu$ can vary due to the chiral anomaly relation. However, the $\chi\omega$ term cannot change the helicity of the magnetic field as can be checked by taking the difference of (36) and (37), and so γ_ω can be assumed constant and taken out of the integral. Then for the $\chi\omega$ term we get

$$\langle \tilde{B}^{\pm*}(\eta, \mathbf{k}) \tilde{v}^\pm(\eta, \mathbf{k}') \rangle = \gamma_\omega k^2 \int_{\eta_0}^{\eta} d\eta' \langle \tilde{v}^{\pm*}(\eta', \mathbf{k}) \tilde{v}^\pm(\eta, \mathbf{k}') \rangle \quad (39)$$

and we need the unequal time correlator for the velocity field.

We expect the fluid velocity at any k mode to be correlated on the eddy turnover time scale $2\pi/kv(\eta, k)$, where $v(\eta, k)$ is the fluid velocity, and to be uncorrelated on longer time scales. This suggests

$$\langle \tilde{v}^{\pm*}(\eta', \mathbf{k}) \tilde{v}^\pm(\eta, \mathbf{k}') \rangle = \langle \tilde{v}^\pm(\eta, \mathbf{k})^2 \rangle (2\pi)^3 \delta^{(3)}(\mathbf{k} - \mathbf{k}'), \text{ for } |\eta - \eta'| < \frac{2\pi}{kv(\eta, k)} \quad (40)$$

and

$$\langle \tilde{v}^{\pm*}(\eta', \mathbf{k}) \tilde{v}^\pm(\eta, \mathbf{k}') \rangle = 0, \text{ for } |\eta - \eta'| > \frac{2\pi}{kv(\eta, k)} \quad (41)$$

where $v(\eta, k)$ is the fluid velocity at length scale $2\pi/k$ at time η . (We will relate $v(\eta, k)$ to $v^\pm(\eta, k)$ in Eq. (55) below.)

Inserting these unequal time correlators in Eq. (39) gives

$$\langle \tilde{B}^{\pm*}(\eta, \mathbf{k}) \tilde{v}^\pm(\eta, \mathbf{k}') \rangle = \gamma_\omega k^2 f(\eta, k) |v^\pm|^2 (2\pi)^3 \delta^{(3)}(\mathbf{k} - \mathbf{k}') . \quad (42)$$

where $f(\eta, k) = \eta - \eta_0$ for $\eta - \eta_0 \leq 2\pi/(kv)$, and $f(\eta, k) = 2\pi/(kv)$ for $\eta - \eta_0 > 2\pi/(kv)$. An example of a smooth function with the same asymptotic properties is

$$f(\eta, k) = S \frac{2\pi}{kv} \tanh\left(\frac{kv}{2\pi S}(\eta - \eta_0)\right) \quad (43)$$

where $S \sim 1$ is a fudge factor. We will adopt this choice for $f(\eta, k)$ in our numerical calculations.

The form of the correlator (42) is based on (39) which is valid at early times when the $\chi\omega$ effect dominates. The correlator will not be valid at later times when the $\chi\omega$ effect becomes sub-dominant, but then the form of the correlator is also not important. Hence we can adopt the form (42) for all times.

So the MHD equations become

$$\partial_\eta |B^+|^2 = 2(-\gamma_D k^2 + \gamma_B k) |B^+|^2 + 2\gamma_\omega^2 k^4 f(\eta, k) |v^+|^2 \quad (44)$$

$$\partial_\eta |B^-|^2 = 2(-\gamma_D k^2 - \gamma_B k) |B^-|^2 + 2\gamma_\omega^2 k^4 f(\eta, k) |v^-|^2 \quad (45)$$

These equations are linear in the quadratic variables $|B^\pm|^2$.

From Eq. (21), the evolution of the ensemble averaged comoving chemical potential is given by

$$\frac{d\Delta\mu}{d\eta} = -c_\Delta \alpha \int \frac{kdk}{2\pi^2} \partial_\eta [|B^+|^2 - |B^-|^2] - \Gamma_F \Delta\mu . \quad (46)$$

Eqs. (44), (45) and (46) are the dynamical equations that we will need to solve after specifying the velocity modes, v^\pm .

B. Fluid Velocity

We consider the scenario of a strong first order phase transition at an early epoch, much earlier than the electroweak phase transition. As bubbles of the new phase grow and collide, the cosmological medium gets pushed and turbulence is generated. The radius of the bubbles at completion of the phase transition defines the length scale at which the fluid is being driven. Let us call this length scale ζ_b . In a non-expanding spacetime, on length scales smaller than ζ_b we

expect a Kolmogorov distribution of velocities, and on larger scales, if we assume a random superposition of constant velocity domains of size ζ_b , we expect a white noise spectrum. In a cosmological setting, we also need to account for Hubble expansion. The largest scale relevant for turbulent flows will be the size of the eddy that circulates at least once per Hubble time. This length scale is $\zeta_H \sim v\eta$ where v is the flow velocity driven by the bubbles. Then the inertial scale is set by the smaller of ζ_b and ζ_H and will be denoted by ζ_i .

The fluid velocity spectrum is given by a power law

$$E_V(\eta, k) = v_i^2(\eta) \left(\frac{k}{k_i(\eta)} \right)^n, \quad (47)$$

where k_i denotes the inertial wavenumber, v_i is the fluid velocity at this scale. On small length scales, $k > k_i$, the Kolmogorov spectrum gives $n = -2/3$, whereas we take a white noise spectrum, $n = 3$, on large length scales, $k < k_i$. (The assumption of white noise on large length scales is not crucial for the main qualitative features in the evolution as these all occur in the Kolmogorov part of the spectrum.) From Eq. (47) we get the velocity at wavenumber k ,

$$v(\eta, k) = v_i(\eta) \left(\frac{k}{k_i(\eta)} \right)^{n/2}. \quad (48)$$

In the radiation era, and on large length scales with $k < k_i(\eta)$, the velocity field does not change (*e.g.* Sec. 7.3.2 of [28]). So

$$v(\eta, k) = v(\eta_0, k), \quad k < k_i(\eta), \quad (49)$$

where η_0 is the time of the phase transition. Combining Eqs. (48) and (49) with $n = 3$, we obtain

$$v_i(\eta) = v_i(\eta_0) \left(\frac{k_i(\eta)}{k_i(\eta_0)} \right)^{3/2}. \quad (50)$$

Now the inertial wavenumber, k_i , is defined by

$$k_i(\eta) = \frac{2\pi}{v_i(\eta)\eta}. \quad (51)$$

When inserted in Eq. (50) we get

$$v_i(\eta) = v_i(\eta_0) \left(\frac{\eta_0}{\eta} \right)^{3/5}. \quad (52)$$

Plugging back into (51) gives [29]

$$k_i(\eta) = k_i(\eta_0) \left(\frac{\eta_0}{\eta} \right)^{2/5}. \quad (53)$$

With these expressions the fluid velocity in Eq. (48) can be written as

$$v(\eta, k) = v_i(\eta_0) \left(\frac{\eta_0}{\eta} \right)^{(3-n)/5} \left(\frac{k}{k_i(\eta_0)} \right)^{n/2}. \quad (54)$$

We will assume that there is no kinetic helicity in the velocity flow and from Eq. (24) write

$$|v^+(\eta, k)| = |v^-(\eta, k)| = \pi k^{-3/2} v(\eta, k). \quad (55)$$

C. Numerical Evolution

We will now solve Eqs. (44), (45) and (46) with the velocity spectra as given in Eqs. (55). We will consider a few different values of $v_i(\eta_0)$ and take $\eta_0 = M_*/T_0$ where $T_0 = 10^{10}$ GeV is the temperature at which the phase transition occurs and $M_* = 6.6 \times 10^{17}$ GeV. At the high temperatures we are considering, e should be the Abelian (hypercharge) gauge coupling constant but, for numerical purposes, we take it to be given by $e = \sqrt{4\pi\alpha}$ in γ_ω and

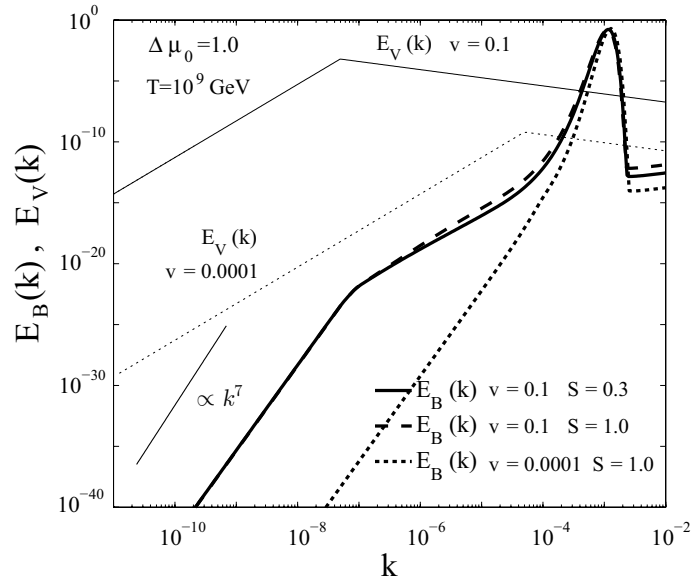


FIG. 3: Plots of the magnetic energy spectrum at $T = 10^9$ GeV for different values of the peak velocity and fudge factor S (see Eq. (43)) exhibit very similar features.

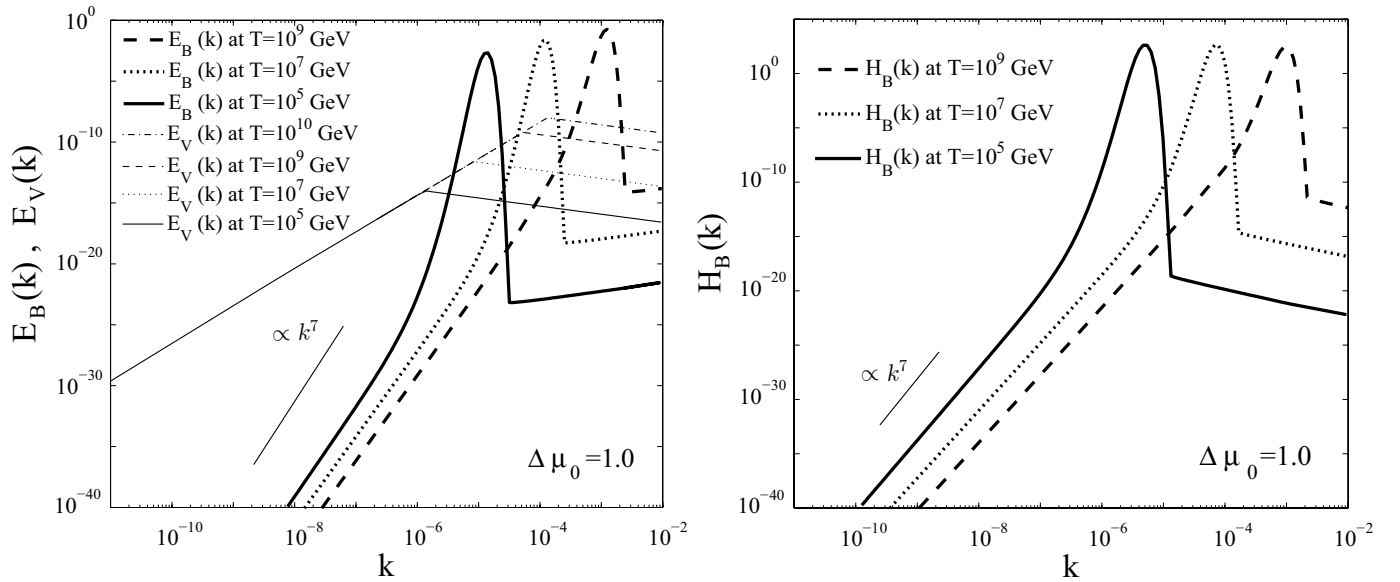


FIG. 4: Evolution when the initial velocity flow is non-helical with $v_i(\eta_0) = 10^{-4}$ and the initial chemical potential is $\Delta\mu_0 = 1$. The left panel shows the power spectra, E_B and E_V , which are normalized to the comoving radiation energy density, $g_*\pi^3/15$. The thick lines are for E_B and the thin lines are for E_V . The spectra are shown at the three different times, $T = 10^9$ GeV (dashed), $T = 10^7$ GeV (dotted) and $T = 10^5$ GeV (solid). The thin dotted-dashed line is the initial velocity power spectrum at $T = 10^{10}$ GeV while the initial magnetic field vanishes. Similarly, the right panel shows the evolution of the magnetic helicity spectrum.

γ_B , where $\alpha = 1/137$. The comoving electrical conductivity is $\sigma = 70$ as in Eq. (19). We consider several different values for the chemical potential at η_0 but focus on $\Delta\mu_0 = 1.0 = \Delta\mu_0^2$. The initial magnetic field is taken to vanish in all cases, as is the flipping rate Γ_F since this is small at temperatures above ~ 80 TeV [23]. Note that the equations of motion are independent of the initial epoch of turbulence but the velocity field in Eq. (54) explicitly contains η_0 , and hence T_0 .

We start by showing the magnetic energy spectrum at a fixed time ($T = 10^9$ GeV) for several different values of the peak velocity and parameter S (defined in (43)) in Fig. 3. The plots show that a sharp peak in the spectrum

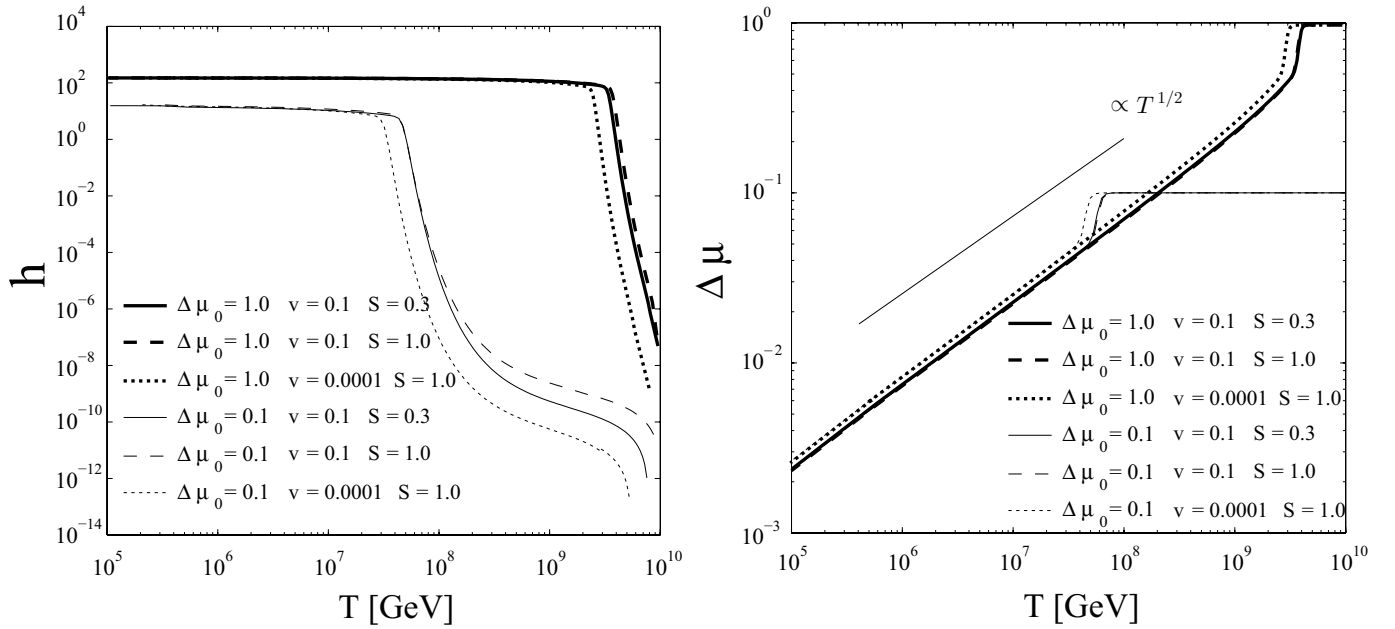


FIG. 5: Evolution of the total helicity (left panel) and the chemical potential (right panel), when the initial velocity flow is non-helical and the initial magnetic field vanishes, for several different parameters.

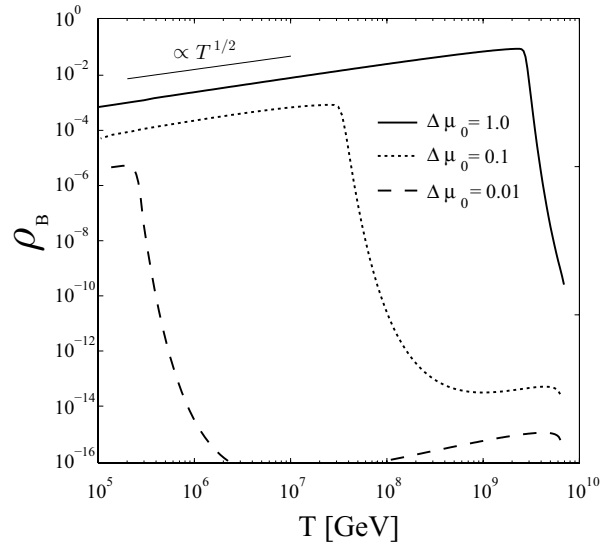


FIG. 6: Evolution of magnetic energy density with temperature for three different values of μ_0 and with $v_i(\eta_0) = 10^{-4}$.

develops and its position and shape are not very sensitive to the input parameters. This can be understood from the evolution equations (44) and (45). For $\gamma_B > 0$, we find that B^- stays small and only B^+ contributes to the magnetic energy density and helicity. At early times, the velocity field acts as a source term for B^+ and the first term on the right-hand side of Eq. (44) is negligible. However, with evolution, the first term becomes more important and the coefficient is negative for $k > \gamma_B/\gamma_D$ and positive for $k < \gamma_B/\gamma_D$. This change in sign implies a peak in the spectrum at $k \approx \gamma_B/\gamma_D \sim e^2 \Delta\mu/2\pi^2$, or on a comoving length scale $4\pi^3/(e^2 \Delta\mu)$. The position of the peak at $k \approx \gamma_B/\gamma_D$ also agrees with our numerical results. We will give a more precise analytical derivation of the peak location in Sec. IID.

The left panel of Fig. 4 represents the evolution of $E_B(k)$ and $E_V(k)$, and the right panel shows the evolution of $H_B(k)$, for $\Delta\mu_0 = 1$ and $v_i = 10^{-4}$. As is evident in Fig. 4, the peak position shifts toward large length scales with evolution. This can be understood by noting that the peak position $\propto \Delta\mu$, and $\Delta\mu$ is a decreasing function of time.

The evolution of the chemical potential and magnetic helicity are shown in the two panels in Fig. 5. The difference

of chemical potential, $\Delta\mu$, decays and becomes smaller, while the total helicity, h , evolves to its asymptotic value

$$h_* = \Delta\mu_0/\alpha c_\Delta. \quad (56)$$

The main contribution to the total magnetic helicity comes from the peak of the helicity spectrum. At this peak, the diffusion and χB terms in Eq. (44) cancel each other. Further evolution occurs since the chemical potential is changing and this shifts the peak position.

The chemical potential difference $\Delta\mu$ has an ‘‘attractor’’ solution – different initial values, $\Delta\mu_0$, all evolve to decay along a common trajectory with $T^{1/2}$ slope (see Fig. 5). The attractor behavior we observe is stronger than the ‘‘tracking’’ observed in [25] where the authors find constant helicity at late times in the case of a single magnetic field mode. Joyce and Shaposhnikov [22] also observed the $T^{1/2}$ decay of $\Delta\mu$; in addition, we find that the coefficient of the decay is independent of the initial value of $\Delta\mu$. Eventually $\Delta\mu$ becomes very small and the magnetic helicity reaches its asymptotic values (56) as given by the chiral anomaly equation. We will obtain a better understanding of these features in the next section.

In Fig. 6 we plot the magnetic energy density as a function of temperature. During the attractor evolution, this gives $\rho_B \propto T^{1/2}$.

Up to now, we have neglected the advection term in the magnetic field evolution. This assumption is certainly valid in the early stages of the evolution when the magnetic field strength is very small and the chemical potential is large. At later times, however, we might expect the advection term to become important. To clarify this issue we compare the advection and χB terms at the peak position after we have analytically understood the evolution in Sec. IID.

Notice in Fig. 4 that the magnetic energy density at the peak is larger than the kinetic energy density. One might expect backreaction of the magnetic fields on the fluid flow to become important in this situation, and the magnetic and kinetic spectra to asymptotically approach equipartition. However, in our case, except for a brief initial phase, the current is proportional to the magnetic field and so the Lorentz force, $\mathbf{j} \times \mathbf{B}$, vanishes. Thus there is no back-reaction of the magnetic field on the fluid flow.

D. Analytical Understanding

In this section we will be able to understand most of the features of the numerical evolution. Our analysis also applies to the scenarios considered in Refs. [22, 25] since the only difference is in the early stages of the evolution. In Ref. [22], $\Delta\mu_0 \neq 0$ and a non-zero initial magnetic field are assumed. In Ref. [25], $\Delta\mu_0 = 0$ and the initial helical seed field is injected during baryogenesis. In the present work $\Delta\mu_0 \neq 0$ and a non-zero seed field is generated due to turbulence and the $\chi\omega$ effect.

The equations to be evolved are (44), (45) and (46). Initially, $B^\pm = 0$ and so only the $\chi\omega$ terms are important. Then

$$|B^\pm(\eta, k)|^2 \approx 2k^4 \int_{\eta_0}^{\eta} d\eta \gamma_\omega^2 f(\eta, k) |v^\pm(\eta, k)|^2 \quad (57)$$

Note that γ_ω has not been pulled out of the time integration because it is proportional to $\Delta\mu$ and this must be evolved according to (46). However, at these early stages, $B^+ \approx B^-$ and the right-hand side of (46) vanishes, and so $\Delta\mu$ and γ_ω are constant. This is also seen in Fig. 5 where the curves of $\Delta\mu$ are flat at the highest temperatures.

The $\chi\omega$ dominated evolution continues until the χB term starts to become important. The transition occurs at time η_1 such that

$$\gamma_B k \int_{\eta_0}^{\eta_1} d\eta f(\eta, k) |v^\pm(\eta, k)|^2 \approx f(\eta_1, k) |v^\pm(\eta_1, k)|^2 \quad (58)$$

where v^\pm are given in Eq. (55). For $\eta > \eta_1$, we can ignore the $\chi\omega$ term.

In the Kolmogorov part of the spectrum, Eq. (54) gives $v^\pm \propto \eta^{-11/15}$ and, assuming $2\pi\gamma_B < 1$, the integral on the left-hand side of Eq. (58) is dominated by the contribution from $\eta \sim 2\pi/k$. A simple estimate then gives

$$\eta_1 \approx \frac{1}{(2\pi\gamma_B)^{15/22}} \frac{2\pi}{k} \quad (59)$$

and this introduces an extra k dependence in $B^\pm(\eta_1, k)$. However, we find $B^\pm(\eta_1(k), k) \propto k^{-1/10}$ in the Kolmogorov part of the spectrum, and this weak dependence will be ignored in what follows. Also, as in Fig. 4, the evolution will lead to a sharp peak in the spectrum, which is the most interesting and dominant feature in the spectrum. In

discussing this peak, we can treat η_1 as being independent of k , since the Kolmogorov spectrum is relatively flat over the width of the peak. So we will simply set $\eta_1 = 0$ from now on. This simplification will not affect the gross features of the evolution.

Ignoring the $\chi\omega$ term, the equation for B^\pm can be written as

$$\partial_\eta |B^\pm| = -\gamma_D k(k \mp k_p) |B^\pm| \quad (60)$$

with

$$k_p \equiv \frac{\gamma_B}{\gamma_D} = \frac{e^2 \Delta\mu}{2\pi^2}. \quad (61)$$

Eq. (60) can be solved and the solution written as the product of an initial amplitude, an exponential amplification factor common to all modes, and a Gaussian spectrum,

$$|B^\pm(\eta, k)| = |B_0^\pm| \exp(\gamma_D K_p^2 \eta) \exp\left[-\gamma_D (k \mp K_p)^2 \eta\right] \quad (62)$$

where the peak of the Gaussian for B^+ is at

$$K_p \equiv \frac{1}{2\eta} \int_0^\eta d\eta' k_p \quad (63)$$

The restriction $k > 0$ implies that B^- is given by the tail of a Gaussian which is peaked at $k = -K_p$. Therefore B^- can be ignored except for $\eta \approx 0$.

Thus the spectrum of B^+ is a Gaussian of width

$$\Delta k \approx \frac{1}{\sqrt{\gamma_D \eta}} \quad (64)$$

which is consistent with the width of the peaks in Fig. 4. It is also interesting to note that the peak gets narrower with time.

Now we can estimate the magnetic helicity

$$h = \int \frac{dk}{2\pi^2} k (|B^+|^2 - |B^-|^2) \quad (65)$$

$$\approx \frac{A}{\sqrt{\eta}} K_p e^{2\gamma_D K_p^2 \eta} \quad (66)$$

where $A = |B_0^+|^2 / \sqrt{2\pi^2 \gamma_D}$. The magnetic energy density is obtained from Eq. (29)

$$\begin{aligned} \frac{1}{2} \langle |\mathbf{B}(\eta, \mathbf{x})|^2 \rangle &= \int \frac{dk}{4\pi^2} k^2 [\langle |B^+(\eta, k)|^2 \rangle + \langle |B^-(\eta, k)|^2 \rangle] \\ &\approx \frac{A}{2\sqrt{\eta}} K_p^2 e^{2\gamma_D K_p^2 \eta} \end{aligned} \quad (67)$$

From the chiral anomaly equation, we also have

$$\Delta\mu = \Delta\mu_0 - c_\Delta \alpha h \quad (68)$$

$$\approx \Delta\mu_0 - \frac{c_\Delta \alpha A}{\sqrt{\eta}} K_p e^{2\gamma_D K_p^2 \eta} \quad (69)$$

As discussed above, during the $\chi\omega$ dominated phase, the helicity stays near zero and $\Delta\mu \approx \Delta\mu_0$. Then $k_p \approx e^2 \Delta\mu_0 / 2\pi^2$ and $K_p \approx k_p / 2 \approx \text{constant}$. In a time $\approx [\gamma_D (\Delta\mu_0)^2]^{-1}$, the exponential in (69) starts to become important. Then the magnetic helicity increases exponentially fast and $\Delta\mu$ rapidly decreases.

The exponential growth of the helicity terminates when it gets close to the asymptotic value h_* , given by Eq. (56). The subsequent evolution can be investigated by setting $h \approx h_*$ in Eq. (66). In order for h to saturate at h_* , the exponent in Eq. (66) has to become nearly constant, $K_p^2 \eta \approx \text{const}$, or

$$K_p \propto \eta^{-1/2}. \quad (70)$$

Then Eqs. (63) and (61) imply

$$k_p \approx K_p \quad (71)$$

and

$$\Delta\mu \propto \eta^{-1/2} \propto T^{1/2} \quad (72)$$

which is the attractor solution seen numerically.

To make these estimates more quantitative, we set

$$K_p \approx k_p = \frac{e^2 \Delta\mu}{2\pi^2} \approx CT^{1/2}, \quad (73)$$

where C is a constant (or, more exactly, a slowly varying function) to be determined. Substituting this into (66) and using $T = M_*/\eta$, we obtain

$$C \approx (2\gamma_D M_*)^{-1/2} (\ln X)^{1/2}, \quad (74)$$

where

$$X = (h_*/AK_p)\sqrt{\eta} \propto \eta. \quad (75)$$

This shows that C has a weak, logarithmic dependence on η .

Comparing Eqs. (66) and (67) and using (73), we can estimate the magnetic energy density in the attractor regime,

$$\frac{1}{2} \langle |\mathbf{B}(\eta, \mathbf{x})|^2 \rangle \approx \frac{1}{2} h_* K_p \approx \frac{C \Delta\mu_0}{2\alpha c_\Delta} T^{1/2}. \quad (76)$$

Note that, apart from the logarithmic factor, the coefficient C in (73) is a constant independent of $\Delta\mu_0$ and of the turbulent velocity spectrum $v^\pm(\eta, k)$. Thus Eq. (76) shows that the attractor magnetic energy density is (roughly) proportional to the initial chiral disbalance $\Delta\mu_0$ and is largely independent of $v^\pm(\eta, k)$. The characteristic length scale of the magnetic field,

$$K_p^{-1} \approx C^{-1} T^{-1/2}, \quad (77)$$

is not sensitive to any of the input parameters.

To get numerical estimates, we evaluated X and C at the lower end of our temperature range, $T = 10^5$ GeV. This is done by solving the transcendental equation (74), after substituting expressions for A (below (66)), B_0^+ (from (57)), η_1 (from (58)), and other relevant quantities. For $\Delta\mu_0 = 1.0$, this gives $X \approx 3.8 \times 10^{16}$, $C \approx 4.5 \times 10^{-8}$, in reasonable agreement with our numerical results. We have verified that for the range of T and $\Delta\mu_0$ that we considered here C does not vary from this value by more than 0.8%.

We now compare the advection term to the χB term at the peak position. The estimate in Eq. (16) shows that the advection term is sub-dominant if

$$v_x \ll \gamma_B \quad (78)$$

where v_x denotes the velocity in physical space. We use Eq. (24) to go to momentum space

$$v_x \sim v(\eta, k) \quad (79)$$

and $v(\eta, k)$ is given in Eq. (54). Now we set $k = K_p = CT^{1/2}$, $\eta = M_*/T$ in (54) to get

$$v(\eta, K_p) = v_{i0} \left(\frac{CM_* v_{i0}}{2\pi T_0^{1/2}} \right)^{n/2} \left(\frac{T}{T_0} \right)^{(3-n)/5+n/4} \quad (80)$$

where $v_{i0} = v_i(\eta_0)$ and $n = -2/3$. Inserting numbers in GeV units $v_{i0} = 10^{-4}$, $C = 4.5 \times 10^{-8}$, $M_* = 6.6 \times 10^{17}$, $T_0 = 10^{10}$ we get

$$v(\eta, K_p) = 6 \times 10^{-5} \left(\frac{T}{T_0} \right)^{17/30} \quad (81)$$

We also have

$$\gamma_B = \frac{K_p}{\sigma} = \frac{CT_0^{1/2}}{\sigma} \left(\frac{T}{T_0}\right)^{1/2} = 6 \times 10^{-5} \left(\frac{T}{T_0}\right)^{1/2} \quad (82)$$

The temperature dependence of v and γ_B are very similar and so whatever relation holds at the initial time, also holds for all (relevant) later times. For a range of parameters we have used in the numerical analysis, $v \lesssim \gamma_B$, and so the advection term is only marginally important. (From Eq. (74) we see that C is only sensitive to the parameter $\gamma_D = 1/\sigma$.) A smaller value of v_{i0} , or a larger value of γ_B due to several chiral particle species contributing to the χB effect, or a higher initial temperature T_0 , can further ensure that the advection term is unimportant. We also note that the advection term becomes negligible when turbulence is eventually dissipated on the relevant scales. However, if the condition $v \ll \gamma_B$ is not satisfied, the advection term will be important and a full numerical analysis will be necessary.

To summarize our understanding, at very early times, only the $\chi\omega$ effect is important and this generates magnetic fields from the assumed turbulence. As these magnetic fields get stronger, the dissipation and χB effects become more important than the $\chi\omega$ effect. These two terms take the initial spectrum produced by the $\chi\omega$ effect, and introduce a Gaussian peak in the spectrum at $k = K_p$ whose amplitude grows exponentially and with width that decreases as $1/\sqrt{\eta}$. At the same time the magnetic helicity h increases exponentially, the magnetic field becomes maximally helical, and $\Delta\mu$ rapidly decreases. The rapid growth of h terminates as it approaches the asymptotic value h_* , and the system enters the attractor regime, in which $K_p \approx k_p \propto T^{1/2}$ and $\Delta\mu \propto T^{1/2}$. This means that the peak of the spectrum continues to evolve to larger length scales. In the attractor evolution, the magnetic helicity stays approximately constant while the magnetic energy density falls off as $T^{1/2}$.

III. CONCLUSIONS

Maximal parity violation in the standard electroweak model suggests that there may have been an asymmetry in the distribution of left- and right-handed chiral fermions in the early universe, so that the cosmic medium was a ‘‘chiral plasma’’. Such a chiral asymmetry has implications for the generation of magnetic fields via the chiral-magnetic and chiral-vorticity effects [16, 17]. The latter effect leads to the production of magnetic fields during a turbulent phase in the chiral plasma, while the chiral-magnetic effect leads to amplification of the magnetic field [22, 25]. These effects are in addition to the generation of magnetic fields during phase transitions [1, 2] and during sphaleron processes responsible for baryogenesis [2, 3, 9–12].

In this paper we have focused on the consequences of the $\chi\omega$ and χB effects. We have investigated the time-dependent solution numerically in an expanding universe but with two assumptions. First we have considered negligible backreaction of the magnetic field on the fluid velocity, and second we have assumed that the advection term is unimportant. These assumptions simplify the analysis because they linearize the MHD equation. However, the analysis is still highly non-trivial because the chiral anomaly equation connects the evolution of the chemical potentials to the total magnetic helicity which is a sum over all magnetic modes.

Neglect of back-reaction is justified by the fact that maximally helical magnetic fields generated by our mechanism are nearly force-free. We have also verified that it is possible to choose parameters such that the advection term is unimportant for the evolution of the magnetic field at the peak of the spectrum. We leave the inclusion of the advection term, and perhaps a full-blown magneto-hydrodynamic analysis, for future work.

Our numerical solutions show that a magnetic field is generated due to the $\chi\omega$ effect in a turbulent chiral plasma. As the field gets stronger, the χB effect becomes important and leads to rapid amplification of the field on a preferred length scale given by $l_B \sim (K_p T)^{-1} \sim 4\pi^3/(e^2 \Delta\mu)$.¹ The $\chi\omega$ effect becomes insignificant at this stage. The amplification period ends when dissipation (magnetic diffusion) becomes important, and the evolution approaches an attractor regime in which the chemical potential difference decreases as $T^{1/2} \propto t^{-1/4}$, with a corresponding shift of power in the magnetic field to larger length scales. The magnetic helicity density h remains nearly constant in this regime, and the magnetic energy density ρ_B decreases as $T^{1/2}$. The attractor solution for $\rho_B(t)$ is proportional to the initial chiral disbalance $\Delta\mu_0/T_0$, where T_0 is the temperature at the phase transition, and has only a weak logarithmic dependence on the magnitude of velocities and on the spectrum of turbulent motion of the plasma. The coherence length scale of the field is largely independent of both $\Delta\mu_0/T_0$ and the turbulence spectrum.

The attractor regime ends at $T_F \sim 80$ TeV, when helicity flipping becomes important. The magnetic energy density at this point is $\rho_B \sim 10^{-3}(\Delta\mu_0/T_0)\rho_r$ where ρ_r is the energy density in radiation, and the coherence length is

¹ In this section we use the physical, rather than ‘comoving’ value for the chemical potential difference $\Delta\mu$.

$l_B \sim 10^5 T_F^{-1}$, which corresponds to the present comoving scale of 10^4 cm. At $T < T_F$, chirality flipping will reduce $\Delta\mu/T$ and shift the peak to yet larger length scales as in Ref. [25]. When the temperature drops to ~ 0.1 MeV, electron-positron pairs annihilate, resulting in a sudden decrease of the electrical conductivity, σ , by a factor $\sim 10^{-9}$. Analysis similar to that in Sec. IID suggests that a sudden decrease in σ at a time when $\Delta\mu = 0$ will decrease K_p and thus increase the coherence scale. In addition, the width of the Gaussian peak in the spectrum will also increase. Further growth of the coherence length may be caused by the inverse cascade in the decaying MHD turbulence (see, e.g., [30, 31] and references therein). All these effects combined could shift the present coherence length into the range of astrophysical interest. We hope to discuss the evolution of the spectrum through the various cosmological epochs separately.

In addition to the time-dependent analysis we have solved the MHD equations for a steady state solution. This analysis points to the estimate in Eq. (A15) for the initial field generated by the cosmic turbulence.

Acknowledgments

We thank Avi Loeb and Oleg Ruchayskiy for useful comments. TV is grateful to Tufts Institute of Cosmology and to the Institute for Advanced Study, and AV thanks ASU for hospitality. TH thanks the ASU Advanced Computing Center for computing support. This work was supported by DOE at ASU, and NSF at Tufts University.

Appendix A: Steady state solutions

To obtain the steady state solutions, we set $\partial_t \mathbf{B} = 0$ in Eq. (14) and assume that the velocity field is stationary, $\partial_t \mathbf{v} = 0$.

1. Negligible advection

We first consider the case when the advection term, $\nabla \times (\mathbf{v} \times \mathbf{B})$, is small compared to the other terms. Then Eq. (14) reduces to

$$\gamma_D \nabla^2 \mathbf{B} + \gamma_\omega \nabla \times \boldsymbol{\omega} + \gamma_B \nabla \times \mathbf{B} = 0, \quad (\text{A1})$$

or

$$\nabla \times [-\gamma_D \nabla \times \mathbf{B} + \gamma_\omega \boldsymbol{\omega} + \gamma_B \mathbf{B}] = 0, \quad (\text{A2})$$

Then

$$-\gamma_D \nabla \times \mathbf{B} + \gamma_\omega \boldsymbol{\omega} + \gamma_B \mathbf{B} = \nabla \phi, \quad (\text{A3})$$

where ϕ is any scalar function. However, the divergence of the left-hand side vanishes and hence we find $\phi = 0$. So the equation reduces to

$$-\gamma_D \nabla \times \mathbf{B} + \gamma_\omega \boldsymbol{\omega} + \gamma_B \mathbf{B} = 0. \quad (\text{A4})$$

In Fourier space

$$\mathbf{B} = \int \frac{d^3 k}{(2\pi)^3} \mathbf{B}_k e^{i\mathbf{k} \cdot \mathbf{x}}, \quad (\text{A5})$$

$$\mathbf{v} = \int \frac{d^3 k}{(2\pi)^3} \mathbf{v}_k e^{i\mathbf{k} \cdot \mathbf{x}}. \quad (\text{A6})$$

Inserting in Eq. (A4) gives

$$-i\gamma_D \mathbf{k} \times \mathbf{B}_k + i\gamma_\omega \mathbf{k} \times \mathbf{v}_k + \gamma_B \mathbf{B}_k = 0, \quad (\text{A7})$$

The dot product of this equation with \mathbf{k} gives

$$\mathbf{k} \cdot \mathbf{B}_k = 0, \quad (\text{A8})$$

and a dot product with \mathbf{v}_k gives

$$(-i\gamma_D \mathbf{v}_k \times \mathbf{k} + \gamma_B \mathbf{v}_k) \cdot \mathbf{B}_k = 0. \quad (\text{A9})$$

Therefore

$$\mathbf{B}_k = F(\mathbf{k}) \mathbf{k} \times (-i\gamma_D \mathbf{v}_k \times \mathbf{k} + \gamma_B \mathbf{v}_k). \quad (\text{A10})$$

To determine the scalar function $F(\mathbf{k})$, insert into Eq. (A7) and obtain

$$F = \frac{-i\gamma_\omega}{\gamma_B^2 - \gamma_D^2 k^2}. \quad (\text{A11})$$

Therefore

$$\mathbf{B}_k = \frac{-i\gamma_\omega}{\gamma_B^2 - \gamma_D^2 k^2} \mathbf{k} \times (-i\gamma_D \mathbf{v}_k \times \mathbf{k} + \gamma_B \mathbf{v}_k). \quad (\text{A12})$$

If we also assume that the fluid is incompressible, we get

$$\mathbf{B}_k = \frac{-i\gamma_\omega}{\gamma_B^2 - \gamma_D^2 k^2} [\gamma_B \mathbf{k} \times \mathbf{v}_k - i\gamma_D k^2 \mathbf{v}_k], \quad \text{if } \mathbf{k} \cdot \mathbf{v}_k = 0. \quad (\text{A13})$$

We now return to our approximation in this section, namely to ignore the advection term. As discussed at the end of the previous section, this is justified for small fluid flow velocities and small length scales. Our solution shows that there is another situation when it is fair to ignore the advection term. Suppose the spectrum of velocities is dominated by a single mode. Then the advection term in Fourier space is $\mathbf{k} \times (\mathbf{v}_k \times \mathbf{B}_k)$ and this vanishes when we use the solution in Eq. (A12).

The solution (A12) simplifies in the large wavelength limit, $\mathbf{k} \rightarrow 0$. Then

$$\mathbf{B}_k = -i \frac{\gamma_\omega}{\gamma_B} \mathbf{k} \times \mathbf{v}_k, \quad (\text{A14})$$

or

$$\mathbf{B} = -\frac{\gamma_\omega}{\gamma_B} \boldsymbol{\omega} = -\frac{\mu_L + \mu_R}{2e} \boldsymbol{\omega}. \quad (\text{A15})$$

This can also be seen directly from Eq. (14) because we have discarded the advection term and the dispersion term becomes negligible on large length scales. So the steady state solution is given by

$$\mathbf{J}_{\chi\omega} + \mathbf{J}_{\chi B} = 0, \quad (\text{A16})$$

which leads to Eq. (A15).

To get an estimate for the magnetic field strength with coherence scale L , we assume

$$|\boldsymbol{\omega}_L| \sim \frac{v_L}{L}. \quad (\text{A17})$$

This gives

$$B \sim -\frac{\mu_L + \mu_R}{2eL} v_L. \quad (\text{A18})$$

In a time-dependent situation with $\mathbf{B} = 0$ initially, we can expect a field of strength (A15) to develop on a time scale

$$\tau_L \sim L/\gamma_B. \quad (\text{A19})$$

This estimate follows by taking the ratio of the $\chi\omega$ term in the evolution equation, $\sim \gamma_\omega \omega/L$, and the asymptotic value of the magnetic field $\sim (\gamma_\omega/\gamma_B)\omega$. In a turbulent flow, individual eddies are not expected to persist much longer than a single revolution time, $\sim \omega_L^{-1}$. This is longer than τ_L , provided that

$$v_L < \gamma_B. \quad (\text{A20})$$

Note that in this regime, the advection term in (14) is small compared to the χB term, so the neglect of advection is justified.

If v_L is given by the Kolmogorov spectrum

$$v_L \propto v_t \left(\frac{L}{t} \right)^{1/3}, \quad (\text{A21})$$

where v_t is the velocity on a cosmological length scale, and assuming that $v_t \sim 1$ and $(\mu_L + \mu_R) \sim T$, we have

$$B \sim -\frac{T}{2eL^{2/3}t^{1/3}}. \quad (\text{A22})$$

Inserting numbers suitable for the electroweak scale, we obtain the magnetic field on the length scale L ,

$$B_L \sim \frac{10^{18}}{(LT_{\text{EW}})^{2/3}} \text{ G}, \quad (\text{A23})$$

where $T_{\text{EW}} \sim 100 \text{ GeV}$.

2. Negligible diffusion

We now find the steady-state solution with the advection term but without the diffusion term. Now the steady state equation is

$$\nabla \times (\mathbf{v} \times \mathbf{B}) + \gamma_\omega \nabla \times \boldsymbol{\omega} + \gamma_B \nabla \times \mathbf{B} = 0, \quad (\text{A24})$$

which leads to

$$\mathbf{v} \times \mathbf{B} + \gamma_\omega \boldsymbol{\omega} + \gamma_B \mathbf{B} = \nabla \phi, \quad (\text{A25})$$

where ϕ can be any function, including a (scalar) function of the flow velocity e.g. \mathbf{v}^2 . Unlike the case of diffusion domination, the divergence of the left-hand side does not vanish and we cannot argue away ϕ .

By taking scalar and vector products of \mathbf{v} with Eq. (A24) we find the solution

$$\mathbf{B} = -\frac{\gamma_\omega}{\gamma_B(\gamma_B^2 + v^2)} [(\mathbf{v} \cdot \boldsymbol{\omega}') \mathbf{v} - \gamma_B \mathbf{v} \times \boldsymbol{\omega}' + \gamma_B^2 \boldsymbol{\omega}'], \quad (\text{A26})$$

where

$$\boldsymbol{\omega}' = \boldsymbol{\omega} - \frac{1}{\gamma_\omega} \nabla \phi. \quad (\text{A27})$$

To determine ϕ we impose $\nabla \cdot \mathbf{B} = 0$. This gives the equation for ϕ ,

$$\partial_i \left[\frac{(\delta^{ij} + u^i u^j)}{1 + \mathbf{u}^2} \partial_j \Phi \right] - \left[\nabla \times \left(\frac{\mathbf{u}}{1 + \mathbf{u}^2} \right) \right] \cdot \nabla \Phi = S, \quad (\text{A28})$$

where $\mathbf{u} = \mathbf{v}/\gamma_B$, $\Phi = \phi/\gamma_B$ and

$$S = \gamma_\omega \nabla \cdot \left[\frac{(\mathbf{u} \cdot \boldsymbol{\Omega}) \mathbf{u} - \mathbf{u} \times \boldsymbol{\Omega} + \boldsymbol{\Omega}}{1 + \mathbf{u}^2} \right], \quad (\text{A29})$$

with $\boldsymbol{\Omega} = \nabla \times \mathbf{u}$. The parameters γ_ω and γ_B in the above equations are defined in Eq. (15).

Eq. (A28) can be re-written in terms of the metric

$$g^{ij} = (1 + \mathbf{u}^2)(\delta^{ij} + u^i u^j). \quad (\text{A30})$$

Then the equation looks like a Klein-Gordon equation in a curved background with an $\boldsymbol{\Omega} \cdot \nabla \Phi$ coupling and a source term.

The solution of (A28) can be inserted into the above expression for \mathbf{B} in Eq. (A26) and that will be the steady state solution in the case of negligible diffusion.

The advection term is important for large velocities, in particular, for $v \gg \gamma_B$, where γ_B is the parameter in the χB effect. In this case, the second and third terms in the square bracket in Eq. (A26) are suppressed by powers of γ_B and we get the order-of-magnitude estimate

$$B \approx -\frac{\gamma_\omega}{\gamma_B} \hat{\mathbf{v}} \cdot \boldsymbol{\omega} \hat{\mathbf{v}}, \quad (\text{A31})$$

where $\hat{\mathbf{v}}$ denotes a unit vector in the direction of \mathbf{v} . The presence of kinetic helicity is crucial for this estimate to be non-vanishing. Assuming helical flow with $\mathbf{v} \cdot \boldsymbol{\omega} \sim v\omega$, we get

$$B \sim -\frac{\gamma_\omega}{\gamma_B} \omega, \quad (\text{A32})$$

which coincides with the order of magnitude estimate in the case of negligible advection, Eq. (A15).

-
- [1] T. Vachaspati, Phys. Lett. B **265**, 258 (1991).
 - [2] T. Vachaspati, in the Proceedings of the NATO Workshop on "Electroweak Physics and the Early Universe", Sintra, Portugal (1994); Series B: Physics Vol. 338, Plenum Press, New York (1994); [hep-ph/9405286](#).
 - [3] T. Vachaspati, Phil. Trans. Roy. Soc. Lond. A **366**, 2915 (2008) [[arXiv:0802.1533](#) [astro-ph]].
 - [4] A. Kosowsky and A. Loeb, Astrophys.J. **469**, 1 (1996).
 - [5] D. D. Harari, J. D. Hayward, and M. Zaldarriaga, Phys.Rev. **D55**, 1841 (1997).
 - [6] A. Kosowsky, T. Kahniashvili, G. Lavrelashvili, and B. Ratra Phys. Rev. **D71**, 043006 (2005).
 - [7] T. Kahniashvili, Y. Maravin, and A. Kosowsky, Phys.Rev. **D80**, 023009 (2009).
 - [8] L. Pogosian, A. P. S. Yadav, Y. -F. Ng and T. Vachaspati, Phys. Rev. D **84**, 043530 (2011) [Erratum-ibid. D **84**, 089903 (2011)] [[arXiv:1106.1438](#) [astro-ph.CO]].
 - [9] J. M. Cornwall, Phys. Rev. D **56**, 6146 (1997) [[hep-th/9704022](#)].
 - [10] T. Vachaspati, Phys. Rev. Lett. **87**, 251302 (2001) [[astro-ph/0101261](#)].
 - [11] C. J. Copi, F. Ferrer, T. Vachaspati and A. Achucarro, Phys. Rev. Lett. **101**, 171302 (2008) [[arXiv:0801.3653](#) [astro-ph]].
 - [12] Y. Z. Chu, J. B. Dent and T. Vachaspati, [arXiv:1105.3744](#) [hep-th].
 - [13] C. Caprini, R. Durrer and T. Kahniashvili, Phys. Rev. D **69**, 063006 (2004) [[astro-ph/0304556](#)].
 - [14] T. Kahniashvili and B. Ratra, Phys. Rev. D **71**, 103006 (2005) [[astro-ph/0503709](#)].
 - [15] T. Kahniashvili and T. Vachaspati, Phys. Rev. D **73**, 063507 (2006) [[astro-ph/0511373](#)].
 - [16] A. Vilenkin, Phys. Rev. D **20**, 1807 (1979).
 - [17] A. Vilenkin, Phys. Rev. D **22**, 3080 (1980).
 - [18] A. Vilenkin and D. A. Leahy, Astrophys. J. **254**, 77 (1982).
 - [19] D. E. Kharzeev and A. Zhitnitsky, Nucl. Phys. A **797**, 67 (2007) [[arXiv:0706.1026](#) [hep-ph]].
 - [20] D. E. Kharzeev, J. Phys. G G **38**, 124061 (2011) [[arXiv:1107.4004](#) [hep-ph]].
 - [21] E.W. Kolb and M.S. Turner, *The Early Universe* (Addison-Wesley, Reading, MA, 1990).
 - [22] M. Joyce and M. E. Shaposhnikov, Phys. Rev. Lett. **79**, 1193 (1997) [[astro-ph/9703005](#)].
 - [23] B. A. Campbell, S. Davidson, J. R. Ellis and K. A. Olive, Phys. Lett. B **297**, 118 (1992) [[hep-ph/9302221](#)].
 - [24] L. Pogosian, T. Vachaspati and S. Winitzki, Phys. Rev. D **65**, 083502 (2002) [[astro-ph/0112536](#)].
 - [25] A. Boyarsky, J. Frohlich and O. Ruchayskiy, Phys. Rev. Lett. **108**, 031301 (2012) [[arXiv:1109.3350](#) [astro-ph.CO]].
 - [26] M. S. Turner and L. M. Widrow, Phys. Rev. D **37**, 2743 (1988).
 - [27] G. Baym and H. Heiselberg, Phys. Rev. D **56**, 5254 (1997) [[arXiv:astro-ph/9704214](#)].
 - [28] V. Mukhanov, Cambridge, UK: Univ. Pr. (2005) 421 p
 - [29] K. Jedamzik and G. Sigl, Phys. Rev. D **83**, 103005 (2011) [[arXiv:1012.4794](#) [astro-ph.CO]].
 - [30] R. Banerjee and K. Jedamzik, Phys. Rev. D **70**, 123003 (2004) [[astro-ph/0410032](#)].
 - [31] L. Campanelli, Phys. Rev. Lett. **98**, 251302 (2007) [[arXiv:0705.2308](#) [astro-ph]].